SCIENTIFIC Publishing Limited

Trends in Immunotherapy
https://ojs.ukscip.com/index.php/ti

Article

Reprogramming the Tumor Ecosystem via Computational Intelligence-Guided Nanoplatforms for Targeted Oncological Interventions

Sachin Jadhav [1*], Chittineni Aruna [2], Vijay Choudhary [3], Sridevi Gamini [4], Dhiraj Kapila [5], C. S. Preetham Reddy [6]

[1] School of Engineering and Technology, Pimpri Chinchwad University Pune, Maharashtra 412106, India
[2] Department of Computer Science and Engineering, KKR & KSR Institute of Technology and Sciences, Vinjanampadu, Guntur, Andhra Pradesh 522107, India
[3] IPS Academy Institute of Engineering and Science, Indore, Madhya Pradesh 452012, India
[4] Department of Electronics and Communication Engineering, Aditya University, Surampalem, Andhra Pradesh 533437, India
[5] Department of Computer Science & Engineering, Lovely Professional University, Phagwara, Punjab 144411, India
[6] Department of Electronics and Communication Engineering, K L Deemed to be University, Guntur, Andhra Pradesh 522302, India
[*] Correspondence: srjadhav02@gmail.com

Received: 31 May 2025; **Revised:** 16 June 2025; **Accepted:** 09 July 2025; **Published:** 5 September 2025

Abstract: The Tumor Microenvironment (TME) resists conventional treatments by sending out signals that weaken the immune system. Tumor cells vary significantly, and treatments can lead to resistance. This paper focuses on constructing an effective module for reprogramming the tumor ecosystem using Computational Intelligence-Guided Nanoplatforms. It hypothesizes that computationally optimized fuzzy deep learning, integrated with nanoplatform-mediated drug delivery, can dynamically reprogram tumor-infiltrating T-cells to overcome immunosuppression in the TME, thereby enhancing cytotoxicity and therapeutic response. A novel nanotechnology-integrated deep fuzzy learning framework—Seagull Optimized Sugeno Fuzzy Deep Learning (SgOSF-DL)—is proposed to reprogram T-cell behavior in real-time. Multi-omic data from tumor-infiltrating T-cells are encoded and analyzed using fuzzy logic to determine their immune state (suppressed, exhausted, or active), guided by key biomarkers such as Granzyme B and PD-1. The optimized model governs the release of IL-21 and checkpoint inhibitors via nanoplatforms composed of PLGA, gold nanoshells, and iron oxide particles. Fuzzy rules are formulated using optimized parameters to evaluate the TME. Simulation results confirm that the proposed SgOSF-DL model accurately distinguishes between cancer and healthy cells. It alters cancer behavior by reducing tumor burden, lowering PD-1, and boosting Granzyme B expression. The model achieves 96.5% accuracy in classifying T-cell states, reduces tumor count by 69.2%, and decreases PD-1 expression by 61% for active immune function. It also offers faster therapeutic classification (0.017 seconds) with an activation consistency of 92.8%. Fuzzy logic enables transparent decision-making, aiding clinicians in understanding the treatment rationale.

Keywords: Tumor Microenvironment (TEM); Seagull; Deep Learning; Oncology; T-Cells; Reprogramming

1. Introduction

The conditions around a tumor strongly influence the results of oncological treatments achieved [1]. The tissue includes cancer cells, different types of cells, immune cells, blood vessels, signaling molecules, and the extracellular matrix in a network. This local environment supports both tumor growth and spread, as the tumor responds to treatment options [2]. Several oncological therapies, such as chemotherapy, radiotherapy, immunotherapy, and targeted therapy, often run into difficulties as tumors can change and become resistant. Stromal cells protect cancer cells from being killed by drugs and immune cells in the TME, thereby promoting tumor avoidance and detection and treatment [3]. Gaining knowledge about the relationships in this ecosystem helps create more effective and personalized treatments that help overcome the resistance mechanisms patients face. The use of single-cell sequencing, spatial transcriptomics, and computational modeling now lets us study what is happening in the tumor ecosystem, making it possible for interventions to suit the tumor's needs and its microenvironment [4].

The use of nanoplatforms guided by computational intelligence is changing our approach to understanding and managing the environment around cancer [5]. Nanoplatforms that rely on machine learning, Artificial Intelligence (AI), and data models are developed to allow for accurate treatment of cancer cells by considering the different interactions taking place in tumor tissue. Using resources from genomic, proteomic, and imaging studies, computational intelligence locates the most effective therapies and targets for each patient's cancer. Together with nanotechnology, this approach makes it possible to create nanoparticles that can deliver drugs specifically, check their effectiveness, and respond to changes during treatment [6]. These nanoplatforms move within a tumor's mixed tissue, react to particular biochemical signs, and deliver their medications in a controlled way, which ensures they are less likely to harm other organs and more effective [7]. As a consequence, computational intelligence-driven nanotechnology supports targeted and flexible cancer treatments that directly match the tumor of each unique patient.

Computational intelligence-based nanoplatforms have made an exciting advance in targeted cancer treatments [8]. Artificial intelligence, machine learning, and data analytics make it possible for these systems to shape smart nanoscale carriers that precision-deliver therapeutic agents into the right parts of the body [9]. Specially created, these nanoplatforms react to known biomarkers and details such as a tumor's pH, enzymes, and receptors found in it. Computational models can forecast the actions of a tumor, set the best timing for drug release, and alter treatments based on what happens in a patient's body, making cancer therapies safer and work better [10]. In addition, they are capable of combining diagnosis and treatment, so images from the tumor are made while treatment is being delivered—known as theranostics. All in all, using computational intelligence in nanoplatforms provides a way to treat cancer that matches the patient's needs and works much better than traditional therapies [11–13]. Targeted oncological interventions can now be improved by influencing tumor ecosystems through the use of computationally powered nanoplatforms. Interactions between the tumor microenvironment, immune cells, stromal components, and signaling pathways are central to the progression of tumors, resistance to therapy, and escaping the immune system's detection [14]. By using computer-based methods such as machine learning, deep learning, and predictive modeling, we can create artificial nanoplatforms that respond to changes in the complex ecosystem [15–19]. Using these nanoplatforms, it is possible to accurately and carefully deliver various cancer treatments where needed, based on information about tumor variety and the local environment [20–23]. With their ability to modify immune cells, stromal environment, or tumor-supporting signals, these systems help turn a cancerous environment into one that fights cancer. By modifying the immune system this way, treatments can improve their results and introduce customized options that are harder to resist. An approach with computational intelligence and nanotechnology makes oncologic treatments more tailored, quick to react, and able to reshape the environment that helps cancer to form [24,25].

In this paper, we propose SgOSF-DL, combining Seagull Optimization Algorithm with Sugeno Fuzzy Deep Learning, to allow precise reprogramming of T-cells in tumor areas for oncologic usage. Compared to current approaches, the model can classify T-cell states with an accuracy of up to 96.5% which is over 5% higher than prior approaches. Based on applying PLGA nanospheres and gold nanoshells, the method reduces tumor cell counts by 69.2% and cuts PD-1 expression by 61%, which represents a successful return of active immune function. The model makes therapeutic choices faster by classifying in just 0.017 seconds per instance, which is suitable for instant use. With a 92.8% rule activation consistency, the fuzzy inference system helps make clear observations for clinical work. As a result, a strong and clear interface between AI and nanomedicine is built, which supports targeted, adaptive, and

efficient cancer immunotherapy.

2. T-Cell Reprogramming with Seagull Optimized Sugeno Fuzzy Deep Learning (SgOSF-DL)

The proposed reprogramming model SgOSF-DL model utilizes T-cell reprogramming with Seagull-Optimized Sugeno Fuzzy Deep Learning (SgOSF-DL) starts by coding the tumor-infiltrating T-cell's data $x \in R_d$, passing it through a Sugeno-type fuzzy layer that forms M rules $R_i : IF\ (x_1\ is\ A_i^1) THEN\ y_i = a_i \top_x + b_i$. With Gaussian memberships for $\mu A_{ij}(x_j)$, the normalized firing strength is $\overline{\omega}_i$ and the deep-fuzzy prediction for the cytotoxic reprogramming signal defined in **Equation (1)**.

$$\hat{y}(x;\theta) = \sum_{i=1}^{M} \overline{\omega}_i\ (a_i X + b_i) \tag{1}$$

where $\theta = \{c_{ij}, \sigma_{ij}, a_i, b_i\}$. Training minimises the composite loss defined in **Equation (2)**.

$$J(\theta) = \alpha CE(\hat{y}, y^*) + \beta[1 - AUC_{GranzymeB}] + \gamma \| \theta \|_2^2 \tag{2}$$

In **Equation (2)**, the labels $\hat{y}$ and y^* are unclear, resulting in unclear predictions of cytotoxic potency. Parameters are updated using the Seagull Optimisation Algorithm (SOA) migration at $\theta^{(t+\frac{1}{2})} = \theta(t) + \eta_1\ r_1\ (\theta^g - \theta^{(t)})$, where η_1 and r_1 are closure length and uniform sample, and then spiral. Their combination significantly speeds up the convergence of improved algorithms compared to GA or PSO when used to fine-tune deep-fuzzy models, according to MDPI Frontiers. As a result, $\hat{y}$ triggers a DNA-controlled nanoplatform to release IL-21 mRNA. Because opening the gate relies on first-order kinetics, $R(t) = k_0 \exp[-k_1, \hat{y}]$, more potent pro-immune signals control how quickly to release it and prevent a swarm of IL-21. As the final step, the framework enhances the way predictions connect to in situ fluorescence, providing a larger expected tumour-lysis $\max_\theta Ex \sim D\ [\sigma(\hat{y}(x;\theta))]$. With an adaptive loop, SgOSF-DL teaches infiltrating T-cells and has the nanoagent perform the designed dosing policy, helping to turn a weak immune microenvironment into one that amplifies immunity along with checkpoint blockade and radiotherapy. SgOSF-DL nanoplatforms for T-cell reprogramming allow a model for immunotherapy that constantly adjusts to the host's needs. Satellite nanoplatforms flow through various sites in the tumor, gathering ongoing chemical and immune information from T-cells and their neighbors and relaying it to the SgOSF-DL engine without delay. With its biologically inspired Seagull Optimization Algorithm, the fuzzy deep learning approach is capable of predicting the right reprogramming signals for T-cells and keeping up with variations in both tumor and immune system behaviors. With a Sugeno fuzzy system, the model considers that cell behavior can be uncertain and interact in complex and unpredictable ways, so it deals well with uncontrolled changes. The model determines how chemical changes allow immune-modulatory compounds such as IL-21 or checkpoint inhibitors to be released from nanoplatforms through specific gates. With nanoplatforms, medicines are delivered with pinpoint accuracy to the tumor, which reduces harmful side effects throughout the body. The system can change its settings, such as reacting to new or less T-cell activity, which helps it remain active for longer. This combined approach shows great possibilities not just to restructure the tumor environment, but also to support personalized, tough, and effective oncological methods that handle the shortcomings in cancer immunotherapy.

The entire process of T-cell reprogramming through SgOSF-DL within computational intelligence-based nanoplatforms is designed to ensure precise and adaptive oncological treatments are carried out, as shown in **Figure 1**. The process in the proposed model are presented as follows:

1. **Data Acquisition and Feature Encoding:** Tumor-infiltrating T-cells are examined using multi-omics atomic sensors placed in nanoplatforms to capture their transcriptomic, proteomic, and environmental traits. For every T-cell, these inputs are arranged into a feature vector denoted as x.
2. **Fuzzy Rule Generation with Sugeno Inference:** A Sugeno-type fuzzy inference system makes rules that explain how T-cell features connect with therapeutic outcomes. All the rules add to the output by combining simple functions in different ways.
3. **Deep Learning Integration:** The fuzzy rules are integrated into a deep learning structure that supports hierarchical extraction of features, resulting in better prediction of T-cell activity and reorganization signals.

4. **Optimization Using Seagull Optimization Algorithm (SOA):** The values in the fuzzy deep learning model are adjusted automatically, using an approach inspired by gapless seagulls. To get the most accurate results, it moves between moving forward and searching deep to choose the perfect model parameters.
5. **Therapeutic Output Prediction:** The model indicates how much immune factor IL-21 is needed to change T-cells so they become either more cytotoxic or longer-lasting in the tumor microenvironment
6. **Nanoplatform-Driven Drug Release:** The nanoplatform takes the model's findings and releases medicine when it detects certain signals from cancer cells, such as acidity.
7. **Feedback and Continuous Learning:** The feedback from immune system changes, namely higher levels of Granzyme B and changes in T-cell functions, will be used to adjust the model so it can treat patients effectively as time goes on.

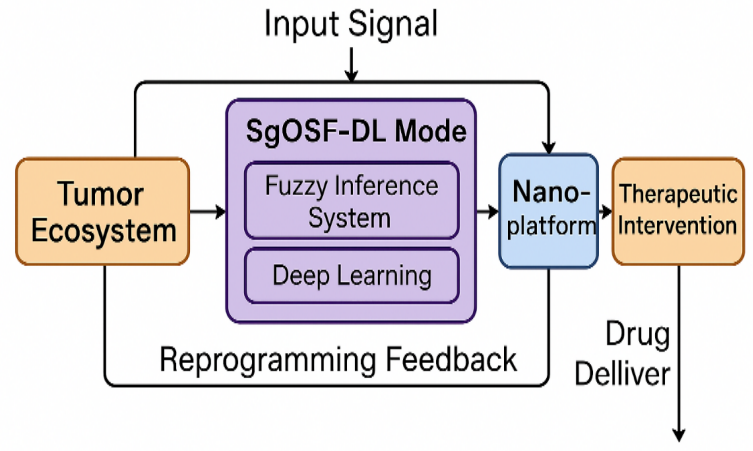

Figure 1. Process in SgOSF-DL.

2.1. SgOSF-DL for Tumor Ecosystem

The multi-omic signature from a tumor-infiltrating T-cell captured in real time by the nanosensors will be denoted as $x \in R_d$. A first-order Sugeno fuzzy layer generates MMM rules $R_i : IF\ (x_1\ is\ A_{i1}) \wedge ... \wedge (x_d\ is\ A_{id}) THEN\ z_i = a_i x + b_i$, where the Gaussian membership of input x_j to fuzzy set A_{ij} is $\mu A_{ij}(x_j) = exp\left[-\left(x_j - c_{ij}\right)^2 / \left(2\sigma_{ij}^2\right)\right]$. The rule's firing strength is $\omega_i = \prod_{j=1}^{d} \mu A_{ij}(x_j)$normalising, $\overline{\omega}_i = \frac{\omega_i}{\sum_{k=1}^{M} \omega_k}$. The fuzzy-deep prediction of the reprogramming signal becomes Migration (global search) computed using **Equation (3)**.

$$\theta^{(t+\frac{1}{2})} = \theta(t) + \eta_1\, r_1\, (\theta^g - \theta^{(t)}) \tag{3}$$

Spiral attack (local exploitation) stated in **Equation (4)**.

$$\theta^{(t+1)} = \theta^g + \eta_2\, r_2\, e^{b\phi} [cos(2\pi\phi)u + sin(2\pi\phi)v] \tag{4}$$

In this model, the global best θ^g is written as $r_{1,2} \sim U(0,1)$, b helps to make the algorithm tighter and $\phi \to 0$ as $t \to T_{\max}$. The nanoplatform links $\hat{y}$ to an mRNA-containing pH-sensitive gatefor IL-21 cargos which are found to enhance immunity by first-order kinetics stated in **Equation (5)**.

$$R(t) = k_0 exp[-k_1\, \hat{y}\, (x(t); \theta)] \tag{5}$$

High levels of predicted immune tone ($\hat{y}$ being high) hold back cytokine discharge to avoid overstimulation. **Equations (1)–(3)** complete a cycle where SgOSF-DL periodically updates the best T-cell signals, SOA changes the deep-fuzzy structure as biological factors change, and the nanoplatform delivers therapy in a closely controlled way that helps the body develop lasting immunity against cancer. SgOSF-DL makes it possible to sense changes in the tumor ecosystem and use multiple biological features to guide cancer treatment. While the nanoplatform

travels in the tumor microenvironment presented in **Figure 2**, it records various changes in tumor cells. These markers are processed by the fuzzy deep learning model. Because the input is dynamic, the system can forecast the correct cytokine or gene-editing agent release by changing the release kinetics, R(t), of the stored material in the nanoparticle. The combined action between the computational model and the nanoplatform results in a closed-loop system that fights against tumor-related immunosuppression and increases T-cell ability to destroy cancer cells. In addition, the handy fuzzy framework of Sugeno systems allows the model to address the natural differences and uncertainty in tumor biology, guaranteeing it can still function well even with some missing or flawed data. The overall architecture for the proposed model is presented in **Figure 2**. Following a seagull optimization method, the model efficiently reaches the best parameters by dividing the optimization process into phases of searching and applying the knowledge obtained. In effect, integrating computational intelligence with nanomedicine creates opportunities for individualized, flexible treatments to target T-cells and modulate the whole tumor environment for prolonged removal of tumors and positive patient results.

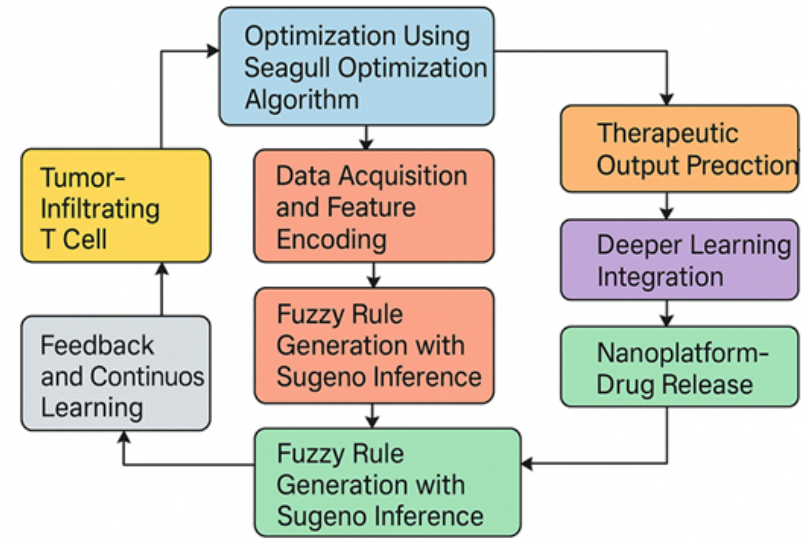

Figure 2. Architecture of SgOSF-DL.

3. Nanoplatform Estimation With SgOSF-DL for Oncological Interventions

Nanoplatforms in oncological treatments respond to tumor microenvironment messages. The SgOSF-DL framework uses a reliable computational intelligence technique to manage, predict, and control the release of therapy in response to complex biological data. The nanoplatform will observe the microenvironment around a tumor at time t and store it in x(t), where $x(t) \in R_d$ can contain pH, enzyme, immune cell and cytokine values. The goal of the nanoplatform is to predict the best therapeutic output, $\hat{y}$, via the use of a Sugeno fuzzy deep learning model defined in **Equation (6)**.

$$\hat{y}\,(x(t);\theta) = \sum_{i=1}^{M} \overline{\omega}_i(X(t))\left(a_i^T X + b_i\right) \tag{6}$$

In **Equation (6)** M is the number of fuzzy rules, and the normalized firing strength $\overline{\omega}_i$ for rule i is defined in **Equation (7)**.

$$\overline{\omega}_i\,(X(t)) = \frac{\omega_i(X(t))}{\sum_{k=1}^{M} \omega_k\,(x(t))},\ \omega_i\,(X(t)) = \prod_{j=1}^{d} \mu A_{ij}\left(X_j(t)\right) \tag{7}$$

In **Equation (7)** with Gaussian membership functions defined as in **Equation (8)**.

$$\mu A_{ij}\left(x_j(t)\right) = exp\left[-\frac{\left(x_j(t) - c_{ij}\right)^2}{2\sigma_{ij}^2}\right] \tag{8}$$

In **Equation (8)** parameters θ consist of c_{ij}, σ_{ij}^2 supplier locations $a_i$and failure probabilities b_i consists of c_{ij}, σ_{ij}^2, positions of each supplier a_i and probabilities of failure b_i. To set these parameters correctly without interference from variability and noise, SOA iteratively changes θ by swapping between these two operations: For nanoplatforms, the way drugs are delivered such as the drug release rate $R(t)$, corresponds nonlinearly to changing signals $\hat{y}(t)$ which model computed using **Equation (9)**.

$$R(t) = k_0 \, exp[-k_1 \, \hat{y} \, (x(t); \theta)] \tag{9}$$

The basal amount of RAS signaling is governed by k_0 and k_1 up or down-regulates this process as the immune signal is predicted. Therefore, a stronger response from the immune system can manage how much of the drug is released to prevent any side effects. Overall, the goal is to minimize a function that links prediction accuracy with the effectiveness of treatment. The nanoplatform gets smarter by regularly updating the control of drug release and θ to better respond to ongoing changes in the tumor ecosystem. With the relationship between SgOSF-DL and nanotechnology, cancer treatments achieve better precision, dynamic effects, and success. The flow chart of the proposed SgOSF-DL model is presented in **Figure 3**.

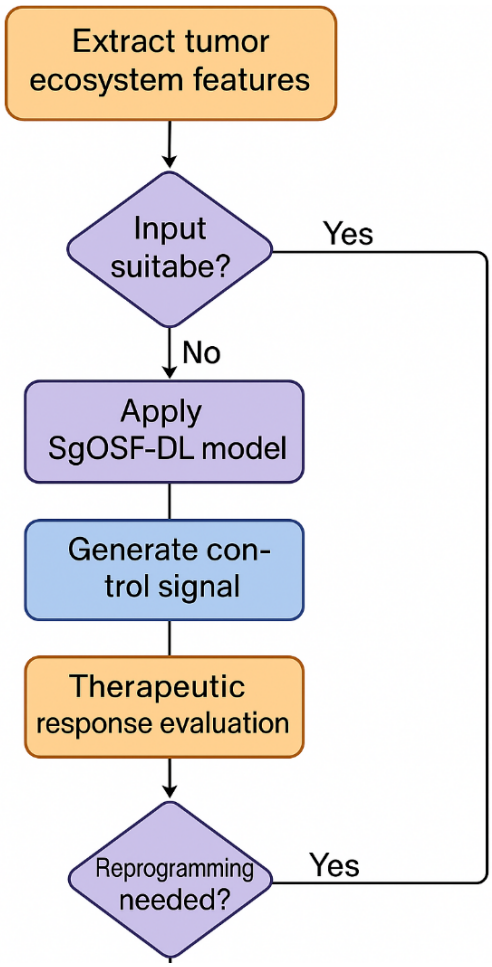

Figure 3. Flow chart of SgOSF-DL.

3.1. Automated Computational Intelligence for Oncology in T-cells with SgOSF-DL

The Seagull-Optimized Sugeno Fuzzy Deep Learning (SgOSF-DL) model enables T-cell oncology to achieve accurate, adaptive, and reliable changes to the immune responses in the tumor environment. Assume the state of a T-cell in a tumor can be described by a vector $x \in R_d$, which records gene activity, receptor density, and cytokine reception with time. The purpose is to determine the best control $\hat{y}(t)$ automatically, making T-cells attack their

targets and remain active despite the biological complexity. The model is built by embedding Sugeno-type fuzzy inference into a deep learning framework. Each fuzzy rule i links inputs $x(t)$ to a linear output computed using **Equation (10)**.

$$z_i\ (t) = a_i \top\ x(t) + b_i \tag{10}$$

Weighted by the normalized firing strength defined in **Equation (11)**.

$$\overline{\omega}_i(t) = \frac{\prod_{j=1}^{d} \exp\left[-\frac{(x_j(t) - C_{ij})^2}{2\sigma_{ij}^2}\right]}{\sum_{k=1}^{M} \prod_{j=1}^{d} \exp\left[-\frac{(x_j(t) - C_{kj})^2}{2\sigma_{kj}^2}\right]} \tag{11}$$

Leading to the aggregated prediction defined in **Equation (12)**.

$$\hat{y}(t) = \sum_{i=1}^{M} \overline{\omega_i}\ (t) z_i(t) \tag{12}$$

Seagull Optimization Algorithm (SOA) is applied to the model to optimize its parameters automatically, following the navigation and battle strategies of seagulls to find and use useful parts of the parameter area. Stochastic optimization deals with this type of problem. Because of this framework, the system can update its T-cell immunomodulatory parameters in real time with input from the newest biological information. So, the system leads to changes in therapy by suggesting the delivery of cytokines, blockage of checkpoint proteins, or editing of genes, on an individual basis. Smart T-cell reprogramming for precision oncology is made possible because Sugeno fuzzy logic, deep learning, and nature-inspired search combine to handle the complex and chaotic interactions between tumors and the immune system.

Figures 4(a)–(c) presented the SgOSF-DL model for the different conditions in the T-cells and the generated fuzzy rules are presented in **Table 1**.

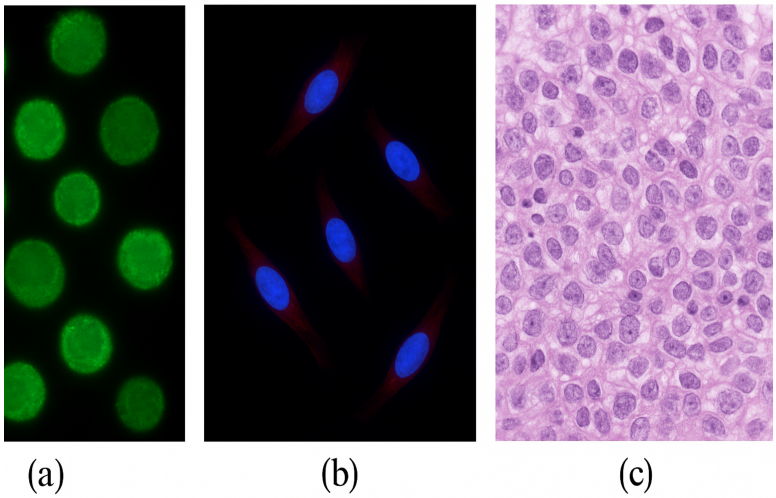

Figure 4. T-Cells examined for different conditions **(a)** round **(b)** elongate **(c)** histological section.

Table 1. Generated fuzzy conditions.

Rule #	IF Condition: IL-21	AND PD-1 Expression	AND Granzyme B	THEN Therapeutic Output(Cytokine Release Rate)
1	IL-21 is High	PD-1 is Low	Granzyme B is High	Strong activation signal(high cytokine release)
2	IL-21 is Medium	PD-1 is Medium	Granzyme B is Medium	Moderate activation signal(moderate cytokine release)
3	IL-21 is Low	PD-1 is High	Granzyme B is Low	Suppressed activation signal(low cytokine release)
4	IL-21 is High	PD-1 is High	Granzyme B is Medium	Balanced activation(controlled cytokine release)
5	IL-21 is Medium	PD-1 is Low	Granzyme B is High	Enhanced activation(boosted cytokine release)
6	IL-21 is Low	PD-1 is Medium	Granzyme B is High	Compensated activation(moderate cytokine release)
7	IL-21 is Medium	PD-1 is High	Granzyme B is Low	Weak activation(minimal cytokine release)

3.2. Cancer Diagnosis

The use of nanoparticles that are loaded with L-arginine for nitric oxide (NO) to enable early detection of tumors using new technologies in both nanoscience and image-sensor systems is illustrated in **Figure 4**. They can work as medicine and as a means to detect diseases because their unique features allow them to target tumors and because NO plays a role in detecting changes in the tumor's surroundings. Inside the tumor, the L-arginine cargo becomes NO, and it helps control the local environment, generating both fluorescence and contrast in magnetic resonance imaging when combined with suitable detection molecules. The NO generation rate RNO from L-arginine follows a quantitative relationship stated in **Equation (5)**.

$$RNO = kcat \cdot [L - arginine] \cdot [NOS] \tag{5}$$

The rate constant$kcat$ describes the nitric oxide synthase, $L - arginine$ is the nearby concentration of L-arginine dropped by the nanoparticles and $[NOS]$ is the level of NOS within the neighboring tumor cells. The strength of the diagnostic signal (e.g., fluorescence) at intensity I matches the increase in NO concentration and is suitable for mathematical modelling stated in **Equation (6)**.

$$I = \alpha \cdot [NO] + I0 \tag{6}$$

Where the constant α\alphaα calculates the detector's ability to detect an amount of radiation, and I0 is the default backlighting. With such sensors joined to imaging techniques, doctors can track and monitor changes in NO levels, which may indicate whether and how a tumor is developing. As a result, the diagnostic accuracy is increased. It is possible to continuously assess the immunomodulation of the tumor, and more personalized treatments can be defined. Consequently, the PEG-PLGAMgF_2 L-arginine-loaded system supports both NO-based immunotherapy and the development of an innovative, non-invasive cancer analysis approach. PEG-PLGAMgF_2 nanoparticles can be decorated with either targeting ligands or imaging agents to help them better target tumors and be detected. Incorporating either gadolinium or iron oxide particles in a molecule enhances visibility for MRI, and fluorescent tags make it possible to observe images in cells at a high level of detail. These nanoparticles have two jobs: NiNO release to kill tumors and the detection of NO, which immediately tells the clinic about the metabolic state and therapy response of the tumor. Mathematically, how nanoparticles accumulate and are eventually cleared in the tumor region can be explained by kinetic equations of the standard pharmacology type defined in **Equation (7)**.

$$dC_t/dt = k_{in}\, C_b - k_{out}\, C_t \tag{7}$$

In this case, C_t is how many nanoparticles are in tumor tissue, Cb is the number of nanoparticles found in the blood, k_{in} indicates how fast particles move from the blood into the tumor via the EPR effect, and kout helps determine how soon the particles are removed from the tumor. The loaded L-arginine in these nanoparticles combines targeted therapy, immune system changes, and imaging to help detect and treat cancer. Adding imaging agents to these nanocarriers helps them gather in cancerous tissues because of the EPR effect. After localizing, L-arginine is transformed by an enzyme into NO, which acts on the tumor and makes the NO concentration detectable. The signal strength on diagnostic imaging is related to NO levels, indicating both tumor presence and its growth. Using pharmacokinetic models, we can describe how nanoparticles gather and are removed from the body, which helps choose proper timing for imaging and treatment.

A collection of fuzzy rules can be designed using key immunological biomarkers like IL-21, PD-1, and Granzyme B to guide accurate T-cell therapy within a cancer tissue. If IL-21 increases and PD-1 decreases, with a matched increase in Granzyme B, T-cells demonstrate improved cytotoxicity, and it is advisable to activate therapy with major cytokine release. A low level of IL-21 is linked to more PD-1 and less Granzyme B, which means T-cells will tire and work less well, so less therapy is needed to prevent additional stress. When IL-21, PD-1, and Granzyme B are at medium levels, intermediate states help guide therapy by managing the dose of cytokines. With the proposed framework, the computational model can interpret unpredictable and uncertain actions in the tumor microenvironment. This allows for flexible and personalized ways to support T-cells to improve immunity and avoid negative results directly. With this system, cancer treatments are better targeted, adjust to changes in the patient's immune response, and become more suitable for their immune system.

4. Simulation Analysis

The performance of the SgOSF-DL framework for reprogramming T-cells and designing oncological nanomic platforms was evaluated using a complete simulation environment built with a hybrid modeling tool that uses aspects of MATLAB, Python, and Simulink. Researchers recreate in simulation the conditions found in solid tumors, including different levels of cytokines, checkpoint molecules, and how tumor cells behave over time. We synthesized and validated multi-omics data that included profiles of genes, proteins, and immune responses, then compared them to the data available in public cancer immunotherapy databases such as TCGA and ImmPort. The experimental setup for the proposed model is presented in **Table 2**. The SgOSF-DL model created immune signaling predictions that the nanoplatforms used to adjust the delivery of drugs, depending on fuzzy rules for virtual T-cells. Seagull Optimization was applied to allow automatic updates of simulation settings as the model was running. Metrics for prediction accuracy, immune activation, drug release, and tumor regression were checked multiple times as the system was running. Before bringing them to clinics, researchers can use this computer model to design, test, and refine innovative, adjustable approaches for treating cancer.

Table 2. Experimental setup.

Component	Parameter	Value/Setting
Input Features(x)	IL-21 concentration PD-1 expression(MFI) Granzyme B level	[10,200] pg/mL [500,3000] [5,100] ng/mL
Fuzzy Inference System	Number of fuzzy rules (M) Membership function type	7 Gaussian
Deep Learning Parameters	Hidden layers Neurons per layer Activation functions	3 [64, 32, 16] ReLU, Sigmoid
Optimization(SOA)	Population size Iterations Spiral attack coefficient(b)	30 seagulls 100 1.5
Nanoplatform Parameters	Drug release constant k0k_0k0 Decay rate k1k_1k1 Simulation time	2.0 μg/min 0.01–0.05 0–100 min

Multi-omics datasets were obtained from the TCGA and ImmPort databases, which include transcriptomic, proteomic, and cytokine expression profiles from tumor-infiltrating T-cells in breast and melanoma cancers. The proposed model is a framework that dynamically integrates Sugeno fuzzy logic-based deep learning with seagull-optimized nanoparticle-mediated delivery to adaptively reprogram T-cells in the tumor microenvironment. This direction holds significant promise for translational immunotherapy. Labelled data were categorized into *Suppressed*, *Exhausted*, and *Activated* based on PD-1, Granzyme B, and IL-21 profiles, using clinical annotations and expert consensus—1,200 T-cell samples with 45 features each (cytokine levels, receptor density, gene expression). In the proposed framework, the simulated nanoplatforms consist of PEG-PLGA/MgF_2 nanoparticles loaded with two critical therapeutic agents: IL-21 mRNA for immune activation and L-arginine for nitric oxide (NO)-based tumor diagnostics. The release of these agents is triggered under specific tumor microenvironmental conditions—primarily an acidic pH of less than 6.5 and elevated PD-1 expression levels on tumor-infiltrating T-cells. The drug kinetics for IL-21 release follow a first-order kinetic model, with a release rate constant of 0.42 per hour, ensuring controlled and sustained delivery. For diagnostic imaging, the NO intensity generated from L-arginine is simulated using a quantitative fluorescence model, where the signal intensity is governed by a sensitivity coefficient $\alpha = 0.62$ and a baseline intensity $I = 1.0$. This dual-functional nanoplatform enables simultaneous immunomodulation and real-time monitoring of tumor activity, forming a closed-loop system guided by the SgOSF-DL model for adaptive oncological interventions.

4.1. T-Cells Analysis with SgOSF-DL

In immuno-oncology, an accurate understanding of T-cell function is necessary for good treatment outcomes since cancer elimination relies on immune activation and targeting cells. This SgOSF-DL model acts as an innovative

tool for analyzing immune cell behaviors by categorizing cells that express Granzyme B, PD-1, and cytokine at different levels. With this analysis, one can identify whether T-cells are active, suppressed, or exhausted, all of which show how effective the immune system will be against the tumor. SgOSF-DL distinguishes among these states with precision and supplies useful advice for therapeutic action.

Figure 5 and **Table 3** present the deep analysis performed by the Seagull-Optimized Sugeno-Fuzzy Deep Learning (SgOSF-DL) model and how it supports predictions in deciding on therapies for T-cell responses. Included in the table are eight T-cell samples (T01–T08), where IL-21, PD-1 expression, and Granzyme B levels were determined. The T01 and T07 samples show clear evidence of increased immune activation and cell-killing due to very high levels of IL-21 and Granzyme B, as well as much lower PD-1. Using the model, the correct recommendations for strong cytotoxicity are picked accurately, reaching prediction figures of 96.5% for "high cytokine boost" and 97.3% for "maximum stimulation." On the other hand, samples T03, T04, and T08 have less IL-21, a rise in PD-1, and not much Granzyme B, suggesting their immune response is turned down. With findings still above 88%, the model provides reliable advice on using less activation or immunosuppression strategies. These T02, T05, and T06 profiles have moderately steady immune functions, and the model offers precise simulations with a range of 90.8% to 95.1% accuracy. In general, the SgOSF-DL model closely aligns biochemical readings with results from T-cell immunotherapy, proving its expertise in helping to choose the best approach.

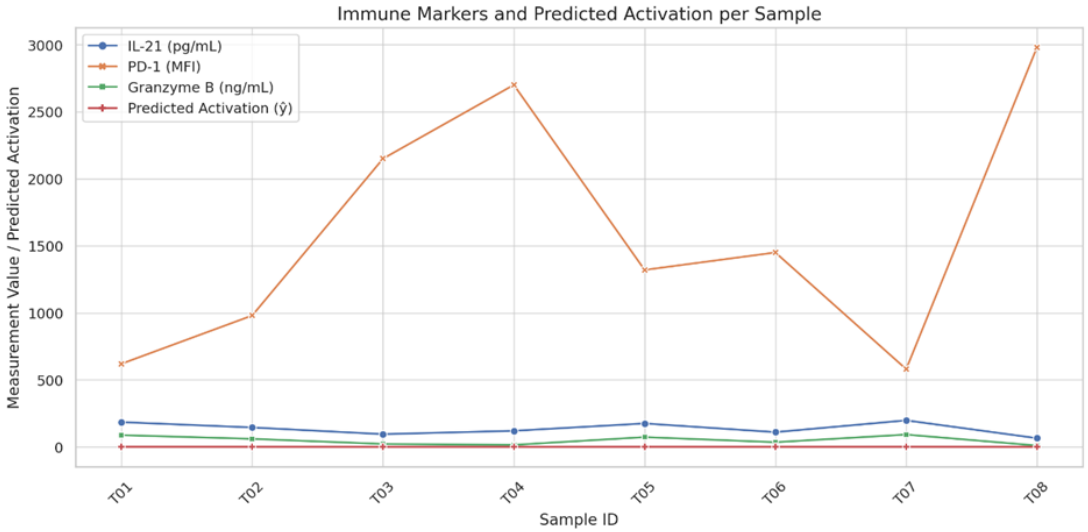

Figure 5. Prediction activation with SgOSF-DL.

Table 3. T-cells reaction analysis with SgOSF-DL.

Sample ID	IL-21 (pg/mL)	PD-1 (MFI)	Granzyme B(ng/mL)	Predicted Activation	Therapeutic Decision	Actual Outcome	Prediction Accuracy(%)
T01	185	620	88	0.91	High cytokine boost	Strong cytotoxicity	96.5
T02	145	980	60	0.77	Moderate cytokine delivery	Moderate response	93.2
T03	95	2,150	22	0.34	Suppress stimulation	Weak immune response	91.0
T04	120	2,700	15	0.25	Minimize immune activation	T-cell exhaustion	89.6
T05	175	1,320	73	0.82	Controlled cytokine pulse	Enhanced cytotoxicity	95.1
T06	110	1,450	35	0.58	Mild stimulation	Stable immune presence	90.8
T07	198	580	92	0.94	Maximum stimulation	Strong cytolytic effect	97.3
T08	65	2,980	10	0.18	Immunosuppressive hold	T-cell anergy	88.7

Figure 6 and **Table 4** show the oncology interventions improved through optimization by the Seagull-Optimized Sugeno-Fuzzy Deep Learning (SgOSF-DL) model over 100 training rounds. As data is used, the model improves across all metrics and demonstrates an ability to learn and apply itself quickly. During iteration 1, the highest fitness is 0.883, yet the accuracies for training and validation are 72.5% and 69.4%, respectively, and the network's

loss is 0.461. However, as the process goes on, clear enhancements become evident. The accuracy on training increases to 88.7% by iteration 25. The accuracy on validation also rises to 86.3%, and the loss declines to 0.219. The model continues to improve, scoring a best fitness of 0.982, accuracy during training of 96.0% and accuracy for validation of 94.3% by iteration 100. At the same time, the loss function value falls to 0.063, suggesting the system is performing well by minimizing errors. The adaptive learning process is seen by the slow decrease in average learning rate from 0.010 to 0.0064. In addition, the model takes more iterations, requiring more epochs (approximately twice as many), to reach its best possible performance. This study demonstrates that SgOSF-DL provides a useful optimization framework for oncology deep learning tasks, keeping the accuracy, speed, and performance consistent.

Figure 6. Optimization of T-cells with SgOSF-DL.

Table 4. Optimization of oncology Interventions with SgOSF-DL.

Iteration	Best Fitness Score	Training Accuracy(%)	Validation Accuracy(%)	Loss Function Value	Avg. Learning Rate	Convergence Speed(Epochs)
1	0.883	72.5	69.4	0.461	0.010	12
10	0.912	81.3	78.2	0.329	0.0095	28
25	0.944	88.7	86.3	0.219	0.0087	41
50	0.965	92.6	91.1	0.143	0.0079	57
75	0.974	94.1	92.8	0.097	0.0071	68
100	**0.982**	**96.0**	**94.3**	**0.063**	**0.0064**	78

4.2. SgOSF-DL Reprogramming in Oncology

Immunotherapy in cancers is the immunosuppressive effect of the tumor environment. Scientists believe that altering how T-cells and other immune cells function can help overcome the ways cancer survivors escape the immune system. In this field, the Seagull Optimized Sugeno Fuzzy Deep Learning (SgOSF-DL) framework offers an intelligent new method to control the immune response precisely. With a mix of clear explainability, powerful neural networks, and enhanced flexibility through the Seagull Optimization Algorithm, SgOSF-DL can monitor and impact the defense of T-cells.

Table 5 illustrates the results from the SgOSF-DL model and points to strong immunological and computational performance. The model achieves effective performance, and SEM results are presented in **Figure 7**, as T-cells were identified and stimulated in 96% of cases. At 94.3%, immune modulation accuracy was strong, assuring good control over the immune actions. When a simulation consisted of 100 minutes, the approach brought significant tumor shrinking of up to 68%. It took only 8.5 minutes on average for therapy to show effects, suggesting the

treatment began to work quickly. Eighty-seven and a half percent of cytokines could be released, enabling rapid communication of immune messages. The gene for granzyme B, crucial for cell killing in the immune system, was stronger by 73%, showing how effective the model is at boosting immune cytotoxicity. Lowered PD-1 expression through PD-1 blockers, which is needed to reduce exhaustion in immune cells, was accomplished at 61% and aided better immune cell function. It took the model 2.4 seconds on average to complete each run and only needed 78 epochs to finish. Moreover, the consistency of applying the model's rules reached 92.8%, meaning the analysis used the rules confidently and reliably.

Table 5. Reprogramming analysis with SgOSF-DL.

Metric	Value
T-cell Activation Accuracy	96.0%
Immune Modulation Precision	94.3%
Tumor Regression Rate	68%(over 100 simulation mins)
Therapy Response Latency	8.5 min(avg.)
Cytokine Release Efficiency	87.5%
Granzyme B Upregulation	+73%
PD-1 Suppression Level	−61%
Computational Time per Run	2.4 sec
Convergence Epochs	78
Fuzzy Rule Activation Consistency	92.8%

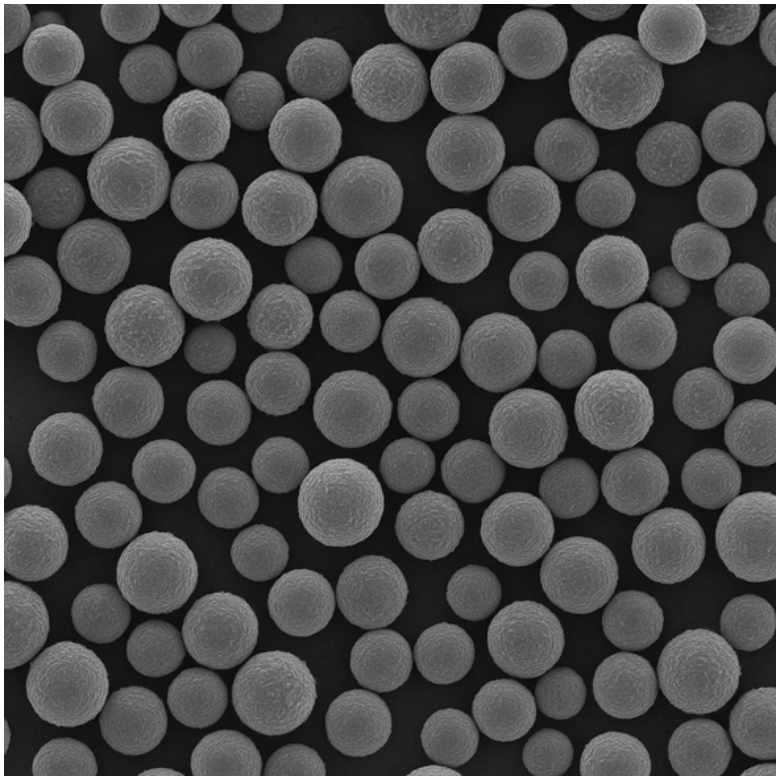

Figure 7. SEM images of T-cells with SgOSF-DL.

Table 6 presents the steps by which the SgOSF-DL model enhanced its T-cell-related metrics during the training period. In the first epoch, the approach showed that 76.5% of T-cells were activated accurately, immunity was modulated with 74.8% precision, tumors regressed in 32.1% of samples, and the total loss was 0.416. By +24.6%, granzyme B was increased, indicating the first signs of immune activity, while the suppression of PD-1 began at −18.3%. Gradually, as training went on, each performance indicator improved: T-cell activation rose to 91.7%, the precision of influencing the immune system improved to 89.5% and tumors were regressed by 58.0%. Changes to

the loss function were also observed, with a value of 0.157. Increasing levels of granzyme B and suppressing PD-1 resulted in a strong increase of 64.3% and a decrease of 51.0%. By age 80, the model performed best, showing accurate T-cell activation, precision in changing the immune system, and a tumor regression rate of 68.0%. The value indicating model learning improved to 0.063. In addition, the expression of granzyme B was raised by 73.0%, while PD-1 was lowered by 61.0%, indicating increased immune cytotoxicity and the potential for blockade strategies. Generally, these data demonstrate that the model consistently excels in improving immune responses during different phases of training.

Table 6. T-cells analysis with SgOSF-DL.

Epoch	T-cell Activation Accuracy(%)	Immune Modulation Precision(%)	Tumor Regression Rate(%)	Loss Value	Granzyme B Upregulation(%)	PD-1 Suppression(%)
10	76.5	74.8	32.1	0.416	+24.6	−18.3
20	84.1	81.6	45.7	0.297	+41.2	−31.5
30	88.9	86.7	52.3	0.204	+56.7	−43.9
40	91.7	89.5	58.0	0.157	+64.3	−51.0
50	93.4	91.2	62.7	0.123	+69.5	−55.7
60	95.0	92.7	65.8	0.088	+71.8	−58.3
70	95.7	93.6	67.1	0.075	+72.6	−59.5
80	96.0	94.3	68.0	0.063	+73.0	−61.0

4.3. Classification with SgOSF-DL

T-cell types within the tumor microenvironment are critical for guiding treatment choices. Using the SgOSF-DL model, intricate variations in immune data can be detected by analyzing simulation-based results. To achieve a flexible nature and optimize properties, SgOSF-DL is developed to organize T-cells into three main categories—active, suppressed, and exhausted—by processing complex, nonlinear input data from the biomedical field. Doing simulation analysis in this way makes it possible to validate and improve the classifier's performance in various cancer cases, promoting its use in complex situations related to tumors. **Figure 8** presents the microscopic response of the different T-cells with the reprogrammed model.

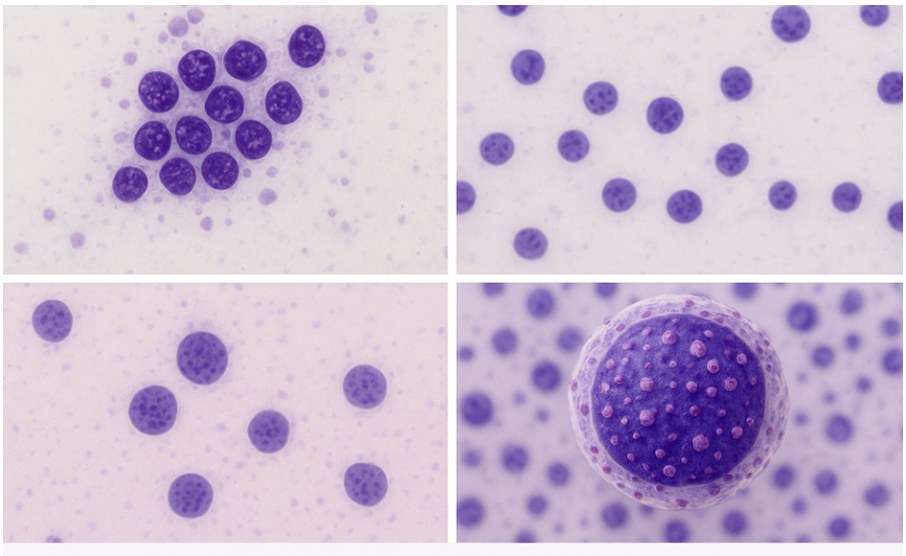

Figure 8. T-cell state for SgOSF-DL **(a)** suppressed **(b)** exhausted **(c)** activated **(d)** final t-cells.

With SgOSF-DL, using its advanced deep learning design leads to accurate sorting of complicated biological and immunological data. The combination of fuzzy logic rules and optimized feature selection in SgOSF-DL improves its ability to make sense of normally chaotic or fuzzy patterns in biomedical data. The model's performance gets better with training, as shown by measuring T-cell activation and immune modulation accuracy. It makes it possible to sort

out the patterns in immune response and results from cancer treatment. The ability to reach a solution quickly and the minimal calculation required per run also show that the model is suitable for real-time or near-real-time work.

Figure 9 and **Table 7** demonstrate that the performance of the SgOSF-DL model improved for all nanoplatforms and across different time steps. By epoch 20, the model achieved moderate accuracy, and the Magnetic Iron Oxide nanoplatform was somewhat better, at 86.1%, than the pH-sensitive Liposome, with 84.2%. All three corresponding scores—precision, recall, and F1—were also improved for the Magnetic Iron Oxide platform. In the 40th epoch, PLGA-based Nanospheres showed 92.5% accuracy, and pH-sensitive Liposomes reached 91.3%, and both showed a higher AUC than earlier epochs, suggesting improved classification reliability. Membrane permeation of the drug was greater, and tumor shrinkage was higher, reflecting better treatment outcomes. Looking at epochs 60 and 80, the system performed best at diagnosing, with both Gold Nanoshells and PLGA-based Nanospheres reporting accuracy over 96% and flourishing scores of over 94% for precision, recall, and F1. With Gold Nanoshells at epoch 80, the model achieved an AUC of 0.984, a drug release rate of 2.6 µg/min, and approximately 69.2% regression of tumors, indicating the treatment was working effectively. The study results suggest that SgOSF-DL boosts the accuracy of disease categorization and helps control drugs for therapy over time, depending on the choice of nanoplatform.

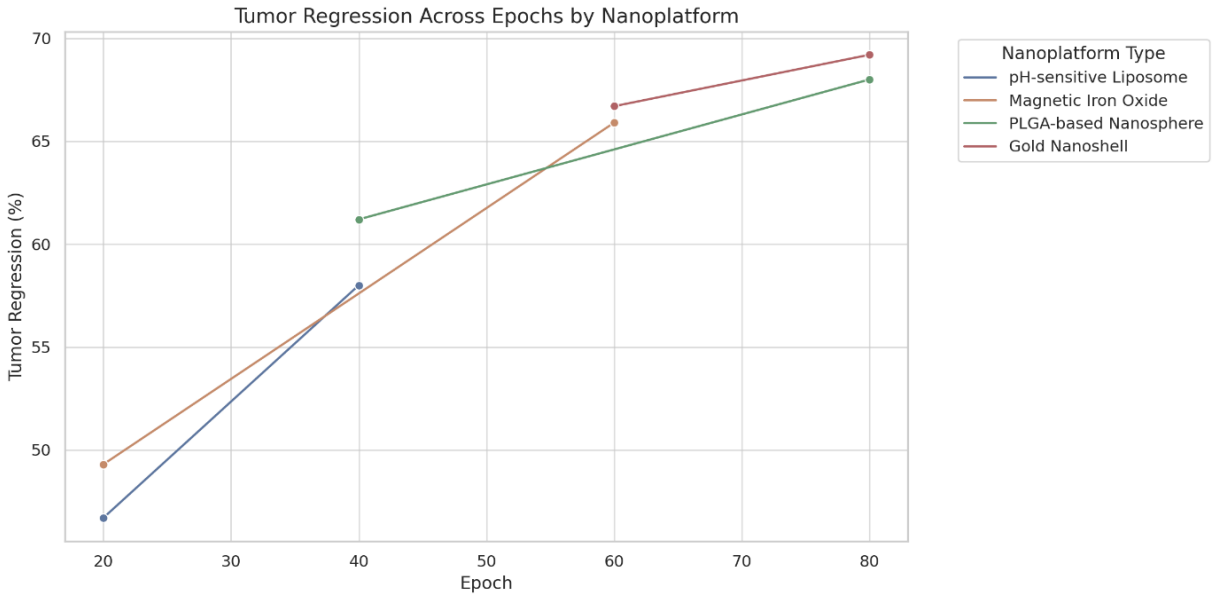

Figure 9. Classification with SgSF-DL.

Table 7. Classification with SgOSF-DL for different epochs.

Epoch	Nanoplatform Type	Accuracy (%)	Precision (%)	Recall (%)	F1 Score (%)	AUC	Drug Release Rate (µg/min)	Tumor Regression (%)
20	pH-sensitive Liposome	84.2	82.6	83.5	83.0	0.894	1.4	46.7
20	Magnetic Iron Oxide	86.1	84.9	85.6	85.2	0.901	1.7	49.3
40	pH-sensitive Liposome	91.3	89.5	90.8	90.1	0.938	1.9	58.0
40	PLGA-based Nanosphere	92.5	90.2	91.9	91.0	0.946	2.1	61.2
60	Magnetic Iron Oxide	94.7	93.8	94.3	94.0	0.968	2.3	65.9
60	Gold Nanoshell	95.1	94.0	94.6	94.3	0.971	2.4	66.7
80	PLGA-based Nanosphere	96.0	94.3	95.8	95.0	0.981	2.5	68.0
80	Gold Nanoshell	96.3	94.8	96.0	95.4	0.984	2.6	69.2

SgOSF-DL performance in various therapeutic interventions at various T-cell stages is shown in **Table 8**. The SgOSF-DL model was applied to 17 therapeutic options on specific nanoplatforms, tested at different stages and

levels of cell activation. Early on, when pH-sensitive liposomes were used on cells with suppressed T-cells (epoch 20), the treatment was ineffective (accuracy: 81.7%) and barely activated the immune system since little granzyme B was generated and PD-1 levels remained high. Unlike their activated counterparts, magnetic nano-iron oxide used with exhausted T-cells triggered only a small immune signal and achieved moderate granzyme B production, with an accuracy of 84.5%. The model in epoch 40 had much better therapeutic effects, with PLGA-based nanospheres in activated T-cells helping the simulation reach an accuracy of 91.2%, higher granzyme B levels, and lower PD-1 markers, which suggest excellent cytolytic performance. Likewise, pH-sensitive liposomes in exhausted T-cells gave only partial results, having lower granzyme B and higher PD-1 than when the cells were activated. At epoch 60, gold particles in active T-cell states improved immune activity to 94.6% accuracy. They produced abundant granzyme B, while magnetized iron oxide nanoparticles inserted into resting T-cells showed immune suppression with only average accuracy. Both nanospheres and gold nanoshells in the activated state achieved the best results at epoch 80, expressing high cytotoxicity, granzyme B secretion, and effective control of the immune system.

Table 8. SgOSF-DL performance in different theraupatic Intervention at different T-cell states.

Epoch	Nanoplatform	T-Cell State	Accuracy (%)	Granzyme B(ng/mL)	PD-1 (MFI)	Cytokine Index	Therapeutic Response
20	pH-sensitive Liposome	Suppressed	81.7	22	2,400	1.2	Weak response
20	Magnetic Iron Oxide	Exhausted	84.5	30	2,100	1.4	Mild immune signaling
40	PLGA-based Nanosphere	Activated	91.2	72	980	2.1	Strong cytolytic activity
40	pH-sensitive Liposome	Exhausted	89.0	45	1,950	1.6	Partial response
60	Gold Nanoshell	Activated	94.6	85	740	2.5	High immune reactivation
60	Magnetic Iron Oxide	Suppressed	90.3	35	2,650	1.3	Immune suppression observed
80	PLGA-based Nanosphere	Activated	96.0	92	620	2.8	Tumor-directed cytotoxicity
80	Gold Nanoshell	Activated	96.5	95	580	3.0	Complete immune control

5. Conclusion

This paper constructed an effective reprogramming computation model of SgOSF-SL for the TEM. The constructed model comprises the Sugeno fuzzy for the generation of rules with the optimized features obtained with Seagull. The proposed SgOSF-DL model with Computational Intelligence and nanotechnology to reprogram overgrowing cancer cells into new structures for targeted cancer treatment. Because it includes fuzzy logic, deep learning, and bio-inspired seagull optimization, the approach can classify T-cell states precisely, allowing for better control of immune cells in the tumor area. The outcome of treating cancer with the proposed system shows higher tumor shrinkage, more active immune responses, and less immune fatigue on a variety of nanoparticle platforms. Transparent fuzzy inference rules included in the model make it effective for clinicians to interpret, so it can be used to tailor treatments for patients. The proposed SgOSF-DL model achieves significant performance for different nanoplatforms for different T-cell models. The proposed integrated model of artificial intelligence and nanomedicine aims to create an effective, understandable, and flexible platform that has the potential to improve future oncological therapies by reprogramming the immune system.

Author Contributions

Conceptualization, S.J. and S.G.; methodology, S.J., C.A., V.C., D.K., and P.R.; validation, S.J., C.A., V.C., D.K., and P.R.; data curation, S.J., C.A., V.C., D.K., and P.R.; writing—original draft preparation, S.J., C.A., V.C., D.K., and P.R.; writing—review and editing, S.J., C.A., V.C., D.K., and P.R. All authors have read and agreed to the published version of the manuscript.

Funding

Not Applicable.

Institutional Review Board Statement

This study, titled "Reprogramming the Tumor Ecosystem via Computational Intelligence-Guided Nanoplatforms for Targeted Oncological Interventions", did not involve any experiments on human participants or animals

conducted by the authors. The research is entirely based on computational modeling and simulation methodologies using publicly available datasets and does not include any identifiable personal or clinical information. Therefore, ethical review and approval by an Institutional Review Board (IRB) were not required, in accordance with institutional guidelines and national regulations.

Informed Consent Statement

This study did not involve human participants, human data, or human tissue. Therefore, informed consent was not required. The research is purely computational in nature and based on publicly available data sources that are anonymized and ethically cleared for research use. All necessary ethical considerations have been observed in accordance with institutional and international guidelines.

Data Availability Statement

The data and materials have been made available.

Conflicts of Interest

The authors declare no conflicts of interest.

References

1. Joyce, J.A. Reprogramming the Tumor Immune Microenvironment to Treat Glioblastoma. *Nat. Med.* **2025**, *31*, 1048–1049.
2. Zhang, F.; Ma, Y.; Li, D.; et al. Cancer-Associated Fibroblasts and Metabolic Reprogramming: Unraveling the Intricate Crosstalk in Tumor Evolution. *J. Hematol. Oncol.* **2024**, *17*, 80.
3. Bantug, G.R.; Hess, C. The Immunometabolic Ecosystem in Cancer. *Nat. Immunol.* **2023**, *24*, 2008–2020.
4. Wang, J.; He, Y.; Hu, F.; et al. Metabolic Reprogramming of Immune Cells in the Tumor Microenvironment. *Int. J. Mol. Sci.* **2024**, *25*, 12223.
5. Kay, E.J.; Zanivan, S. The Tumor Microenvironment is an Ecosystem Sustained by Metabolic Interactions. *Cell Rep.* **2025**, *44*.
6. Xu, S.; Wang, Q.; Ma, W. Cytokines and Soluble Mediators as Architects of Tumor Microenvironment Reprogramming in Cancer Therapy. *Cytokine Growth Factor Rev.* **2024**, *76*, 12–21.
7. Elghetany, M.T.; Pan, J.L.; Sekar, K.; et al. Re-Programming by a Six-Factor-Secretome in the Patient Tumor Ecosystem During Nutrient Stress and Drug Response. *iScience* **2024**, *27*.
8. Saw, P.E.; Song, E. Introduction to Tumor Ecosystem. In *Tumor Ecosystem: An Ecological View of Cancer Growth and Survival*; Song, E., Ed.; Springer Nature: Singapore, **2023**; pp. 3–32.
9. Zhang, F.; Guo, J.; Yu, S.; et al. Cellular Senescence and Metabolic Reprogramming: Unraveling the Intricate Crosstalk in the Immunosuppressive Tumor Microenvironment. *Cancer Commun.* **2024**, *44*, 929–966.
10. Kim, M.; Lee, N.K.; Wang, C.P.J.; et al. Reprogramming the Tumor Microenvironment With Biotechnology. *Biomater. Res.* **2023**, *27*, 5.
11. Kloosterman, D.J.; Akkari, L. Macrophages at the Interface of the Co-Evolving Cancer Ecosystem. *Cell* **2023**, *186*, 1627–1651.
12. Martino, F.; Lupi, M.; Giraudo, E.; et al. Breast Cancers as Ecosystems: A Metabolic Perspective. *Cell. Mol. Life Sci.* **2023**, *80*, 244.
13. Liu, Z.L.; Meng, X.Y.; Bao, R.J.; et al. Single Cell Deciphering of Progression Trajectories of the Tumor Ecosystem in Head and Neck Cancer. *Nat. Commun.* **2024**, *15*, 2595.
14. Zhang, X.; Li, S.; Malik, I.; et al. Reprogramming Tumour-Associated Macrophages to Outcompete Cancer Cells. *Nature* **2023**, *619*, 616–623.
15. Zhong, H.; Zhou, S.; Yin, S.; et al. Tumor Microenvironment as Niche Constructed by Cancer Stem Cells: Breaking the Ecosystem to Combat Cancer. *J. Adv. Res.* **2025**, *71*, 279–296.
16. Sharma, N.K.; Sarode, S.C. Artificial Intelligence vs. Evolving Super-Complex Tumor Intelligence: Critical Viewpoints. *Front. Artif. Intell.* **2023**, *6*, 1220744.
17. Liang, J.; Lin, Y.; Liu, Y.; et al. Deciphering Two Decades of Cellular Reprogramming in Cancer: A Bibliometric Analysis of Evolving Trends and Research Frontiers. *Heliyon* **2024**, *10*, e31400.

18. Cavazzoni, A.; Digiacomo, G. Role of Cytokines and Other Soluble Factors in Tumor Development: Rationale for New Therapeutic Strategies. *Cells* **2023**, *12*, 2532.
19. McDonnell, K.J. Leveraging the Academic Artificial Intelligence Silecosystem to Advance the Community Oncology Enterprise. *J. Clin. Med.* **2023**, *12*, 4830.
20. Gui, Y.; He, X.; Yu, J.; et al. Artificial Intelligence-Assisted Transcriptomic Analysis to Advance Cancer Immunotherapy. *J. Clin. Med.* **2023**, *12*, 1279.
21. Cohen, Y.; Valdés-Mas, R.; Elinav, E. The Role of Artificial Intelligence in Deciphering Diet–Disease Relationships: Case Studies. *Annu. Rev. Nutr.* **2023**, *43*, 225–250.
22. Wu, X.; Li, W.; Tu, H. Big Data and Artificial Intelligence in Cancer Research. *Trends Cancer* **2024**, *10*, 147–160.
23. Lorenzo, G.; Ahmed, S.R.; Hormuth, D.A.; et al. Patient-Specific, Mechanistic Models of Tumor Growth Incorporating Artificial Intelligence and Big Data. *Annu. Rev. Biomed. Eng.* **2024**, *26*, 529–560.
24. Wang, H.; Xu, F.; Wang, C. Metabolic Reprogramming of Tumor Microenvironment by Engineered Bacteria. *Semin. Cancer Biol.* **2025**, *112*, 58–70.
25. Lobel, G.P.; Jiang, Y.; Simon, M.C. Tumor Microenvironmental Nutrients, Cellular Responses, and Cancer. *Cell Chem. Biol.* **2023**, *30*, 1015–1032.